J Neurophysiol 105: 2560–2571, 2011.
First published March 9, 2011; doi:10.1152/jn.01061.2010.

Changes in physiological properties of rat ganglion cells during retinal degeneration

Chris Sekirnjak,[1] Lauren H. Jepson,[1] Pawel Hottowy,[2] Alexander Sher,[3] Wladyslaw Dabrowski,[2] A. M. Litke,[3] and E. J. Chichilnisky[1]

[1]*The Salk Institute for Biological Studies, San Diego, California;* [2]*AGH University of Science and Technology, Krakow, Poland; and* [3]*University of California, Santa Cruz, California*

Submitted 7 December 2010; accepted in final form 7 March 2011

Sekirnjak C, Jepson LH, Hottowy P, Sher A, Dabrowski W, Litke AM, Chichilnisky EJ. Changes in physiological properties of rat ganglion cells during retinal degeneration. *J Neurophysiol* 105: 2560–2571, 2011. First published March 9, 2011; doi:10.1152/jn.01061.2010.—Retinitis pigmentosa (RP) is a leading cause of degenerative vision loss, yet its progressive effects on visual signals transmitted from the retina to the brain are not well understood. The transgenic P23H rat is a valuable model of human autosomal dominant RP, exhibiting extensive similarities to the human disease pathology, time course, and electrophysiology. In this study, we examined the physiological effects of degeneration in retinal ganglion cells (RGCs) of P23H rats aged between P37 and P752, and compared them with data from wild-type control animals. The strength and the size of visual receptive fields of RGCs decreased rapidly with age in P23H retinas. Light responses mediated by rod photoreceptors declined earlier (~P300) than cone-mediated light responses (~P600). Responses of ON and OFF RGCs diminished at a similar rate. However, OFF cells exhibited hyperactivity during degeneration, whereas ON cells showed a decrease in firing rate. The application of synaptic blockers abolished about half of the elevated firing in OFF RGCs, indicating that the remodeled circuitry was not the only source of degeneration-induced hyperactivity. These results advance our understanding of the functional changes associated with retinal degeneration.

receptive field; implant; threshold; rods; cones

SEVERAL MAJOR BLINDING DISEASES such as retinitis pigmentosa (RP) are caused by degeneration of photoreceptors, which results in loss of visual signals and major remodeling of the retinal circuitry (Jones et al. 2003; Jones and Marc 2005). Efforts to construct a retinal prosthesis to treat such diseases depend on stimulating retinal neurons that survive the degeneration process in order to transmit artificial visual signals to the brain (Chader et al. 2009; Javaheri et al. 2006; Mokwa et al. 2008; Winter et al. 2007; Yanai et al. 2007; Zrenner et al. 2009). However, the physiological effects of degeneration on surviving retinal neurons are poorly understood.

The P23H transgenic rat is a useful animal model of retinal degeneration (Kolomiets et al. 2010; Salzmann et al. 2006; Sekirnjak et al. 2009). P23H is the opsin mutation responsible for the most common form of human autosomal dominant RP. In P23H rats, photoreceptors degenerate with a time course similar to what is observed in the human condition, and retinal ganglion cells (RGCs) exhibit progressive loss of light responses and increased overall spontaneous activity during the initial phase of degeneration (Sekirnjak et al. 2009). Yet RGCs continue to respond normally to electrical stimulation (Kolomiets et al. 2010; Sekirnjak et al. 2009), raising the possibility that epiretinal prosthetic devices may function well in the degenerated retina. However, fundamental questions remain about how RGC physiology is altered during degeneration.

First, how do the light responses of RGCs change? Prior physiological studies in P23H rats have focused on recordings of the electroretinogram, which have low resolution (see, e.g., Kolomiets et al. 2010; Machida et al. 2000; Yang et al. 2009). In the RCS rat, a different model of retinal degeneration, recordings in the superior colliculus suggest a gradual loss of contrast sensitivity (see, e.g., Pu et al. 2006; Sauve et al. 2001). To understand the effects of degeneration on RGC light responses in P23H rats, we obtained high-resolution receptive field measurements from >600 RGCs at various time points during photoreceptor loss.

Second, do rod and cone photoreceptors degenerate at different rates, and what are the consequences for visual signals in RGCs? Anatomic evidence suggests that rods degenerate more quickly than cones (see, e.g., Chrysostomou et al. 2009; Cuenca et al. 2004). To investigate the changes in rod and cone inputs to RGCs, we used visual stimuli that preferentially activate either rods or cones.

Third, does photoreceptor loss differentially affect light responses in different RGC types? Previous studies have hinted that early in the degeneration process the impact of photoreceptor loss on ON cells may be greater than that on OFF cells in the rd1 mouse (Stasheff 2008) and the RCS rat (Pu et al. 2006; Sauve et al. 2001). We addressed this question in P23H rats by examining responses of simultaneously recorded ON and OFF RGCs.

Fourth, which RGC types generate the increased spontaneous activity observed during the initial phases of degeneration? In a small sample of 11 ON and 14 OFF cells in the rd1 mouse, both cell types showed elevated firing (Margolis et al. 2008). We measured firing rates in several hundred ON and OFF cells over a wide age range to obtain their respective contribution to hyperactivity in P23H retina.

Finally, what is the source of hyperactivity? One possibility is a change in the intrinsic membrane properties that underlie spontaneous firing; another possibility is an increase in synaptic activity or levels of free glutamate. In the rd1 mouse, there is evidence that hyperactivity arises exclusively from synaptic inputs rather than intrinsic properties (Margolis et al. 2008; Margolis and Detwiler 2011). To investigate this question in

Address for reprint requests and other correspondence: E. J. Chichilnisky, Salk Inst. for Biological Studies, 10010 N. Torrey Pines Rd., La Jolla CA 92037 (e-mail: ej@salk.edu).

P23H rats, we measured spontaneous firing in the presence and absence of antagonists that abolish synaptic transmission.

The present work thus reports the detailed functional properties of RGCs in retina undergoing photoreceptor loss, furthering our understanding of the degeneration process at a cellular level.

METHODS

Animals and Retinal Preparation

P23H line 1 (P23H-1) homozygous breeding animals (Sprague-Dawley background) were provided by Dr. Matthew LaVail (University of California-San Francisco School of Medicine, Beckman Vision Center) and were crossed with pigmented wild-type Long-Evans (LE) rats (Harlan, Indianapolis, IN). The resulting offspring were pigmented heterozygous rats with a single P23H transgene allele in addition to the normal two wild-type opsin alleles. These heterozygous animals undergo a slower retinal degeneration process than homozygous animals, and more closely resemble the human genetic condition of RP (a single mutant transgene and 2 normal copies of rhodopsin). Pigmented wild-type LE rats were used as controls. All procedures on animals were approved by the Salk Institute Institutional Animal Care and Use Committee.

Eyes were enucleated after decapitation of animals deeply anesthetized with 12 mg/kg xylazine and 60 mg/kg ketamine HCl. Immediately after enucleation, the eye was hemisected ~1 mm behind the ora serrata under infrared illumination. The anterior portion of the eye and vitreous were removed, and the eye cup was placed in bicarbonate-buffered Ames' solution (Sigma, St. Louis, MO). Pieces of retina 1–2 mm in diameter were separated from the retinal pigment epithelium and placed flat on a multielectrode array (see below), with the RGC layer facing the array. A transparent dialysis membrane was used to hold the retina close to the electrodes. The assembly was then mounted on a circuit board attached to an inverted microscope and continuously superfused with Ames' solution bubbled with 95% oxygen and 5% carbon dioxide at a flow rate of 2–4 ml/min (chamber volume 0.4 ml) and maintained at 30–33°C.

The thin and fragile retinas of P23H animals with severe degeneration [>postnatal day (P)600] were difficult to separate from the retinal epithelium and sclera for multielectrode array recordings. Thus two of the experiments in older P23H retinas were performed with sclera-attached preparations, which precluded the detection of light responses but permitted measurement of spontaneous activity.

Multielectrode Array

The electrode array used for recording and stimulation has been described in detail elsewhere (Litke 1998; Litke et al. 2003; Sekirnjak et al. 2006). It consisted of a hexagonal arrangement of 61 extracellular electrodes used to record action potentials from RGCs and to inject current. Each electrode was formed by a microwell electroplated with platinum before each experiment. Electrode diameter varied between 7 and 16 μm, with a fixed interelectrode spacing of 60 μm. All electrical stimulation was performed with a monopolar configuration (current flow from electrode to distant bath ground wire).

Spontaneous Firing Rates and Spike Amplitudes

A subset of RGCs (between 10 and 23) in each retina were selected for stimulation and recording. Electrodes that recorded multiple similar spikes from different cells were usually excluded. Preference was given to cells with medium and large spike amplitudes to facilitate analysis, but cells with small-amplitude spikes from a given electrode were included if they were apparently produced by a single cell. Spontaneous firing rates in darkness were measured by counting spikes in 30-s windows and dividing the number of spikes by the window length. For each RGC, data from three or four spike counting periods were averaged. Whenever possible, counting periods interleaved throughout the experiment were used to average out fluctuations in firing rate over time. Spike amplitudes were also measured during these data runs. In animals with similar ages, spontaneous rate data were pooled and assigned to an average age. For statistical analysis, the firing rates at each P23H time point were compared with those of wild-type control animals of a similar age.

Receptive Field Analysis and Cell Counts

An optically reduced stimulus from a color cathode ray tube computer display (Sony Trinitron Multiscan E100) with a refresh rate of 120 Hz was focused on the photoreceptors. The intensity was controlled by neutral density filters in the light path. Spatiotemporal receptive fields (RFs) were measured by using a dynamic white noise stimulus in which the intensity of each display primary at each pixel location was drawn randomly and independently over space and time from a binary distribution. The size of the square pixels was selected to accurately capture the spatial structure of ganglion cell RFs (Chichilnisky 2001) and varied between 33 and 66 μm on a side. Each checkerboard stimulus was displayed for time intervals of 16.67, 25, 33.33, or 50 ms.

The voltage signal on each electrode during the white noise presentation was digitized at 20 kHz and stored for off-line analysis. Details of the recording and spike sorting methods are given elsewhere (Litke et al. 2003, 2004). To describe how the cell integrates visual inputs over space and time, the spike-triggered average (STA) stimulus was computed for each RGC (Chichilnisky 2001). An elliptical two-dimensional Gaussian function was fitted to the spatial profile of each STA (Chichilnisky and Kalmar 2002). This Gaussian function provided a quantitative summary of the RF.

Responses to white noise stimuli were collected continuously during several 20- to 30-min recordings. RGCs were counted within each separate period of visual stimulation. Each such period typically yielded ~25–40 distinct cells; cumulative cell counts across 2 or 3 periods yielded ~40–55 unique RGCs.

Measurement of Receptive Field Properties

To compare RFs across animals, we analyzed results from white noise experiments with visual stimulation parameters intended to preferentially activate cones (see below): 30-min duration, colored binary stimuli with display pixel size 44 or 55 μm, refresh interval 16.67 or 25 ms. Data from animals with similar ages were pooled and assigned an average age (results from 2–8 recordings were averaged).

RF properties were measured with a two-step approach. Since the goal was to compare the properties of light-responsive cells in control and P23H retinas, the first step consisted of eliminating all cells without an unambiguous RF. In the second step, three parameters were calculated from the STA for the remaining cells. The procedure is described below.

Step 1a. The signal-to-noise ratio (SNR) of the peak in the time course of the STA contrast was determined for each cell. First, locations of strong light response were identified by computing the root mean square (RMS) values of the STA over time for every location, then identifying those locations at which the RMS value of the STA exceeded 25% of that of the location with the highest RMS value. Then the STA time course was computed by averaging the time course at these locations. The absolute value of the maximum of the STA time course was then divided by a measure of noise: the robust standard deviation of all the intensity values in the STA. In this calculation, only the green display primary was used because it typically drove responses more strongly than the red or blue.

Step 1b. To limit the subsequent analysis to cells with unambiguous RFs, cells with peak SNR values below 0.35 were discarded; the same

threshold was applied to data from control and degenerated retinas. This SNR threshold was selected to yield similar numbers of false positives and false negatives (i.e., cells falsely classified by eye as having a significant RF or not) in a representative sample of 278 cells in 10 retinas.

Step 2a. For cells that remained after the thresholding procedure, the fit function to the STA contrast time course (Chichilnisky and Kalmar 2002) was examined. The peak in the fit function that occurred closest to $t = 0$ and its time of occurrence were measured for each cell, and the SNR was calculated. Cells with invalid fits (negative peak times and peak SNRs <0.001) were discarded to further exclude any cells without valid RFs.

Step 2b. The average peak SNR (for ON and OFF cells separately) was used as a measure of RF strength. RF diameter was defined as the diameter of a circle with the same area as the 1 SD boundary of the Gaussian center profile (Chichilnisky and Kalmar 2002). For each data run, parameters were averaged over all cells, yielding three final STA parameters to describe light responses (RF strength, time to peak, and RF diameter).

Rod- and Cone-Isolating Stimuli

Isolation of light responses driven by rod photoreceptors was achieved by using low stimulus intensities. RFs in scotopic (rod driven) conditions were measured by presenting stimuli with a mean intensity of 5.6 photoisomerizations·rod^{-1}·s^{-1} (calculated using an effective rod collecting area of 1.0 μm^2), which is below the activation threshold for cones (see Rodieck 1998). Recordings were obtained for 30 min using a black-and-white stimulus with a display pixel size of 55 or 66 μm and a refresh interval of 33 or 50 ms. After data collection at the scotopic light level, recordings were obtained at light levels of 1,400, 2,800, or 5,600 photoisomerizations·rod^{-1}·s^{-1}. Because rod photoreceptors begin to adapt (desensitize) at much lower light levels than cones (see, e.g., Schnapf et al. 1987, 1990), high light levels tend to favor the contribution of cones to RGC signals. However, in rats, there is some uncertainty in the degree to which RGC signals are dominated by cone inputs at the light levels used here. In the macaque isolated retina preparation, RGC responses at a light level of ~1,000 photoisomerizations·rod^{-1}·s^{-1} are dominated by inputs from cones, with little or no detectable input from rods (Field et al. 2009). At the same light level, visual detection thresholds in mice are strongly dominated by signals initiated in the cones (Naarendorp et al. 2010). However, in ex vivo recordings from guinea pig retina, rods rather than cones provide the dominant inputs to horizontal cells at this light level (Yin et al. 2006). Whereas the relative strength of rod and cone inputs to rat RGCs at the high light levels used here has not been determined, the data in mice are suggestive, as are the findings on loss of RFs in RGCs presented here (see Fig. 3). Therefore, in what follows, we provisionally refer to the higher light levels as photopic.

In many experiments, 1–2 h had elapsed between data collection at scotopic and photopic light levels. To exclude data from deteriorating preparations, the number of RGCs was compared during photopic and scotopic experiments. If the ratio was smaller than 65%, the data were excluded. On average, this ratio was 87 ± 4% for control animals ($n = 11$) and 89 ± 5% for P23H animals ($n = 19$).

Synaptic Blockers

In a subset of experiments, a cocktail of compounds intended to abolish synaptic transmission was added to the perfusion bath solution. The following inhibitors were used (in μM): 70 6-cyano-7-nitroquinoxaline-2,3-dione (CNQX), 200 2-amino-5-phosphonovaleric acid (APV), 50 2-amino-4-phosphonobutyric acid (APB), 10 strychnine, 100 picrotoxin, and 1,000 kynurenate. The inhibitors were thoroughly dissolved in Ames' solution bubbled with 95% oxygen and 5% carbon dioxide for ~2 h before perfusion into the recording chamber. A minimum drug perfusion time of 10 min was allowed before responses were recorded.

Electrical Stimulation

Focal monopolar stimulation and recording of evoked spikes has been described in detail elsewhere (Sekirnjak et al. 2008, 2009). Briefly, charge-balanced current pulses of 0.05- or 0.1-ms duration were applied through an electrode adjacent to the electrode on which the RGC was recorded. The retina was maintained in darkness during electrical stimulation. Threshold was defined as the current that produced a spike on 50% of stimulus pulses while stimulating at 5–10 Hz. The planar electrode area (πr^2) was used to calculate charge densities. The stimulation artifact of evoked spikes was removed digitally by using recordings during near-threshold stimulation (Sekirnjak et al. 2008).

Data Processing and Reporting

Multielectrode data were analyzed off-line with IGOR Pro. Images were processed in Photoshop and Intaglio. Statistical significance was calculated by performing a nonparametric two-tailed two-sample Wilcoxon-Mann-Whitney test with a criterion of $P < 0.05$. Results are reported in the text as means ± SE unless otherwise noted; all figure graphs show means ± SD.

The sigmoidal fit functions in Fig. 1 are intended as a guide to the eye. A cumulative Gaussian (error function) was used:

$$f(x) = c + a \cdot G(x \cdot b + d) \quad (1)$$

where

$$G(x) = \frac{2}{\sqrt{\pi}} \int_0^x e^{-t^2} dt \quad (2)$$

and a, b, c, and d are parameters fitted to the data.

The fit function in Fig. 4*B* is intended as a guide to the eye. The following function was used:

$$f(x) = a\left(\frac{x}{b}\right)^c e^{-c\left(\frac{x}{b}-1\right)} \quad (3)$$

with the free parameters a, b, and c fitted to the data.

RESULTS

Here we report the functional properties of RGCs from transgenic P23H-1 rats and compare them to those from wild-type LE rats. A total of 27 LE and 32 P23H animals were used. The goal was to investigate the physiological manifestations of degeneration-induced changes occurring between ~P40 and ~P750 in P23H retina. Portions of the data in this study were used in an earlier paper (Sekirnjak et al. 2009).

RGC Receptive Field Properties During Retinal Degeneration

The number of light-responsive RGCs in P23H retinas decreases as retinal degeneration progresses, to nearly zero by age P550 (Sekirnjak et al. 2009). To investigate how photoreceptor loss influences RGC light responses during degeneration, we examined the RFs of RGCs from retinas of animals of various ages. Figure 1, *A* and *B*, illustrates measurements of RFs in control and P23H rats. The visual stimulus consisted of a square lattice of randomly flickering pixels; RFs were identified by reverse correlation of the recorded spike train with this stim-

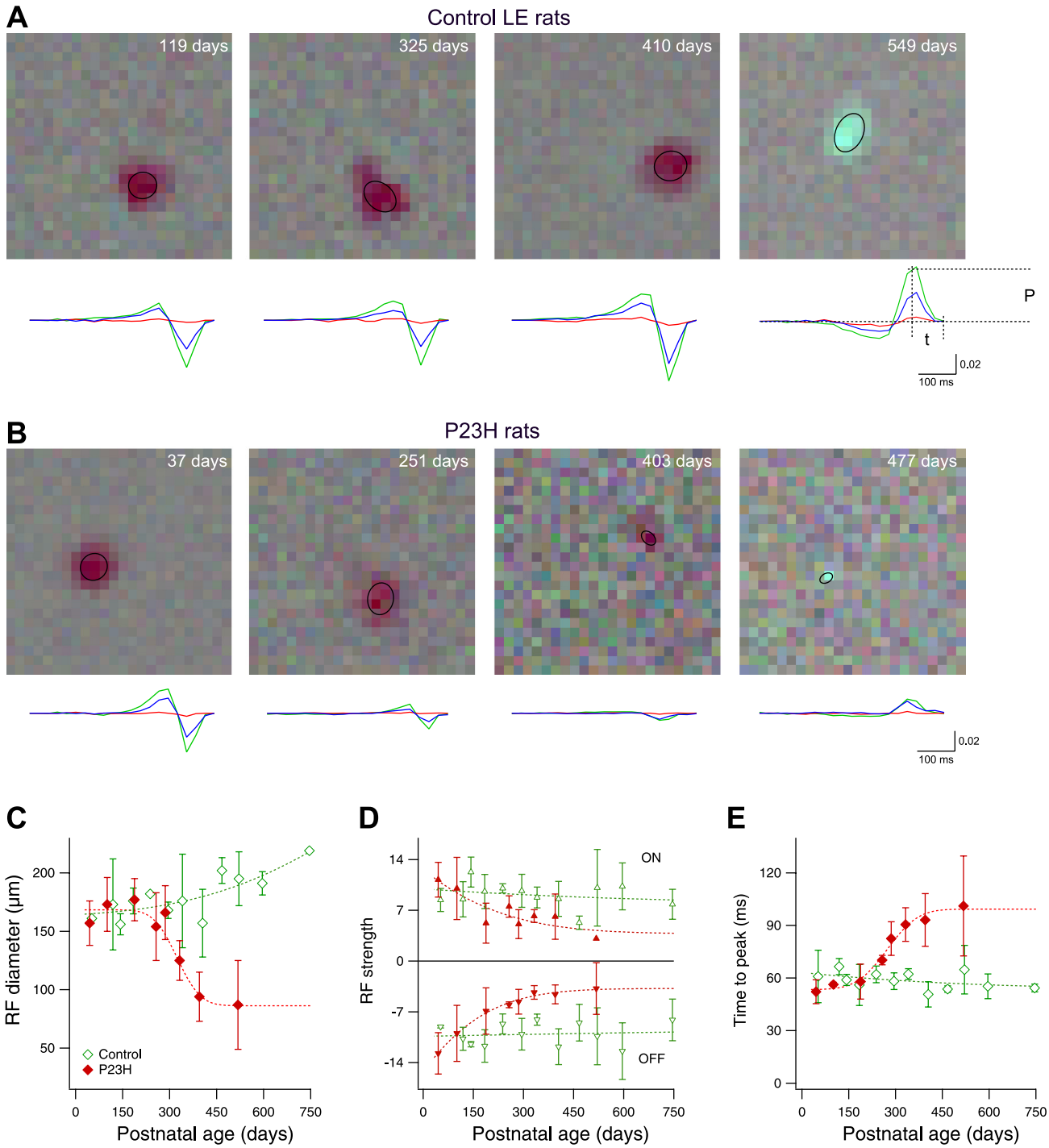

Fig. 1. Receptive field (RF) properties of normal and degenerated retina. *A*: average stimulus observed ~50 ms before a spike in representative examples from 4 control animals of different ages. In the first 3 panels, the regions of darker pixels indicate the RF of OFF ganglion cells; the final panel shows an ON cell. Ellipses represent 1 SD of the Gaussian fit to the spatial profile of each RF. The color line graphs below each RF show the time course of the spike-triggered average (STA) contrast of the red, green, and blue signals (same scale for all graphs) in the 500 ms preceding a spike. To quantify the time course, peak amplitude (*P*) and time to peak (*t*) were used to calculate RF strength and peak time (see below). *B*: representative examples from P23H rats of ages similar to those in *A*. *C*: size of the RF in ganglion cells of control and P23H animals. Data points are averages of all ON and OFF cells in 2–8 retinas; error bars indicate SD. Data points without error bars indicate errors smaller than symbol size. Dashed lines are sigmoidal fits to the data. *D*: strength of the RF in control and P23H rats. This measurement corresponds to the signal-to-noise ratio of the peak amplitude *P* shown in *A*. ON cells (positive peak values, top) and OFF cells (negative peak values, bottom) are shown separately. *E*: time to peak light response. This measurement corresponds to the parameter *t* defined in *A*. Averages of ON and OFF cells are shown.

ulus (see METHODS). The time course of the red, green, and blue STA stimulus is shown below each RF. From Fig. 1*B* it is apparent that in older P23H rats the size of the RF was diminished, and its strength decreased relative to the noise. To quantitatively describe the RF, we measured three parameters: size (diameter of the elliptical fit to the spatial profile of each RF), strength (the peak amplitude of the STA time course relative to the noise), and time of peak light responses.

To compare the size of the RF across animals, Fig. 1*C* shows RF diameter as a function of age. Averages of ON and OFF cells are plotted. Control and P23H retinas showed similar values until P200. In control animals, a slight increase with age was observed, whereas P23H retinas showed a marked decrease. RF size in P23H animals at >P500 was reduced to ~50% of the initial diameter. No significant difference was seen between ON and OFF cells (not shown), although there was a trend toward larger RFs for OFF cells in P23H retinas. It should be noted that in some cases (e.g., Fig. 1*B*, late stages) measurement of RF size was limited by the pixel resolution of the display; thus the smallest RF sizes measured represent an upper bound.

To quantify the strength of light responses, the SNR of the STA time course at its peak time is shown in Fig. 1*D*. The amplitude of the STA relative to noise reflects the strength of the light response relative to background firing. Data from ON cells (peak > 0) and OFF cells (peak < 0) are shown separately. The absolute RF strength was similar in ON and OFF cells (ON-to-OFF ratios were 91 ± 5% in LE rats and 105 ± 9% in P23H rats). LE retinas did not show significant changes of RF strength with age. In P23H retinas, however, RF strength decreased to ~25% of the initial value in OFF cells and ~30% in ON cells. Note that the strength of the RF would likely be underestimated in cases in which the RF size is smaller than the pixel size of the display, later in the degeneration process (e.g., Fig. 1*B*, late stages).

Figure 1*E* shows the time to peak of the STA as a function of age. Averages of ON and OFF cells are plotted. No change was observed in control animals, whereas P23H retinas showed nearly a doubling of the time to peak with age. No significant difference was seen between ON and OFF cells (not shown), although there was a trend toward longer peak times for ON cells in P23H retinas. Note that with advancing age, fewer P23H cells remained light responsive; thus the data points above P400 in Fig. 1, *C–E*, were based on a small number of cells.

In summary, RGCs in P23H retinas exhibited a progressive decrease in RF size and strength, and a slowing of light responses, during and after photoreceptor degeneration.

Effects of Degeneration on ON and OFF Cells

In the rd1 mouse (Stasheff 2008) and RCS rat (Pu et al. 2006), photoreceptor loss appears to affect ON RGCs more than OFF RGCs. We tested for this asymmetry in 1,057 light-responsive cells in LE retina and 705 cells in P23H retina. Relative numbers of ON, OFF, and unresponsive RGCs are shown in Fig. 2*A* for 26 control retinas between P33 and P746. No systematic changes were observed with advancing age, and the total number of light-responsive cells remained constant. Figure 2*B* shows the same measurement in 28 P23H retinas. The fraction of ON cells and OFF cells decreased with age, while the fraction of unresponsive cells increased.

Figure 2*C* compares the number of ON cells in P23H and control retinas, expressed as a percentage of light-responsive cells in each retina. Averaged across age, 35 ± 2% ON cells were identified in 26 control retinas, while 33 ± 3% were found in 28 P23H retinas. No significant difference in the relative numbers of ON cells was apparent between P23H and control animals ($P > 0.6$). A decrease in the fraction of ON cells was observed for the oldest two P23H animals; however, those data were based on one or two ON cells per retina. Notably, similar results were obtained when only rod-mediated light responses were examined (not shown): the fraction of ON cells remained constant at levels similar to those seen in control animals until P300, at which age only ~10% of RGCs showed rod-driven responses (see *Rod-Mediated vs. Cone-Mediated Light Responses*).

In summary, there was no evidence for a differential preservation of ON or OFF RGC responses in P23H retinas.

Rod-Mediated vs. Cone-Mediated Light Responses

Previous studies have suggested that some cone photoreceptors are preserved until after rod photoreceptor degeneration is complete, as assessed by histology and electroretinogram in the P23H rat (Chrysostomou et al. 2009; Cuenca et al. 2004; Machida et al. 2000), in the rd1 mouse (Carter-Dawson et al. 1978), and in the RCS rat (Cicerone et al. 1979). To investigate

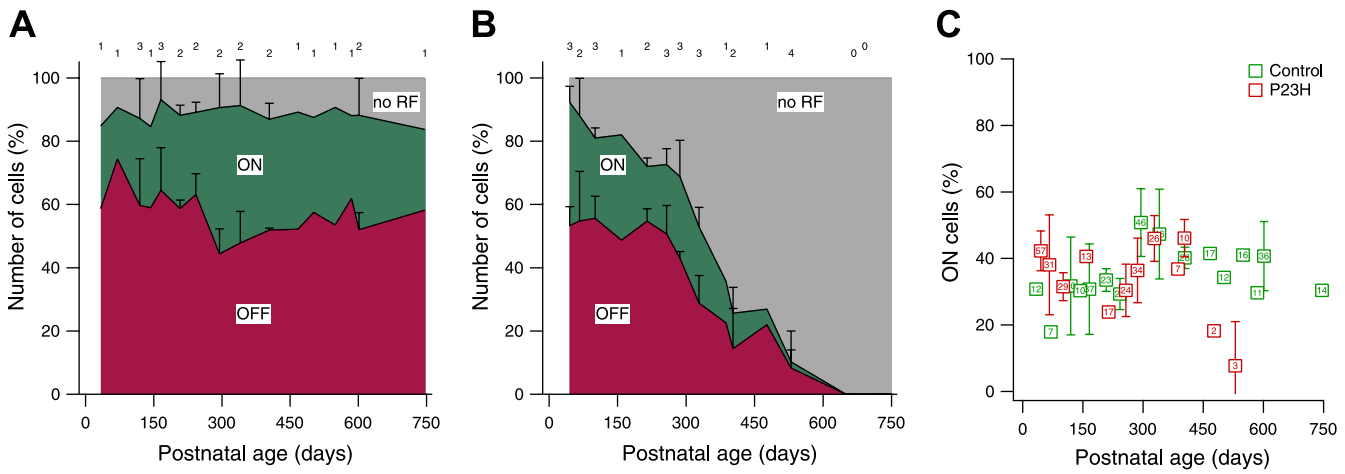

Fig. 2. ON and OFF ganglion cells in control and degenerating retina. *A*: fraction of ganglion cells identified as ON or OFF at different ages in control Long-Evans (LE) retina. Cells without RFs are shown in gray. Each data point indicates % of the total number of ganglion cells per retina. The number of retinas contributing to each data point are shown at *top*. Data points without error bars represent a single retina. Error bars indicate SD. *B*: fraction of ganglion cells identified as ON or OFF at different ages in P23H retina. *C*: number of ON cells as % of light-sensitive cells per retina. Control retinas are compared with P23H retinas. Averages of 2–4 retinas are shown; data points without error bars represent a single retina. Error bars indicate SD. The total number of cells contributing to each data point is shown inside the symbol.

how rod and cone function contribute to RGC light responses, we tested P23H retinas with stimuli that preferentially activated rods or cones. To activate rods, measurements were performed at low light levels (scotopic). To preferentially activate cones, measurements were performed at high light levels (photopic; but see METHODS).

Figure 3*A* shows RFs measured in a P298 control retina. Colored ellipses represent the RFs of ON and OFF cells; colored dots indicate which electrodes recorded spikes. The RFs in Fig. 3*A*, *left*, were measured at photopic light levels: a total of 55 cells were recorded (30 ON cells, 21 OFF cells, and 4 cells with no RF). Data from the same retina stimulated at scotopic light levels are shown in Fig. 3*A*, *right*: the pattern of RFs appeared similar, and a total of 54 cells were recorded (30 ON, 20 OFF, 4 with no RF).

Results from an age-matched (P291) P23H retina are shown in Fig. 3*B*. While the pattern of electrodes with recorded cells was similar under scotopic and photopic conditions, there was a notable absence of RFs at scotopic light levels.

Figure 3*C* summarizes cell counts for 11 control and 19 P23H retinas. The fraction of light-responsive cells in each retina is shown at scotopic light levels in both groups (colored symbols). The functional loss of rod responses preceded the loss of cone responses (black symbols) by ~300 days (photopic data from Sekirnjak et al. 2009).

These findings imply that survival of cones was responsible for the partially preserved light responses in older animals. We thus reexamined the histological data collected previously to locate surviving cones in older P23H retinas (see Fig. 1 in Sekirnjak et al. 2009). We found evidence of a sparse population of outer segments resembling cone remnants in animals as old as P544. An example is shown in Fig. 3*D* for a P23H retina at P344, an age at which no rod-mediated light responses could be detected. Several conelike outer segments are visible (asterisks).

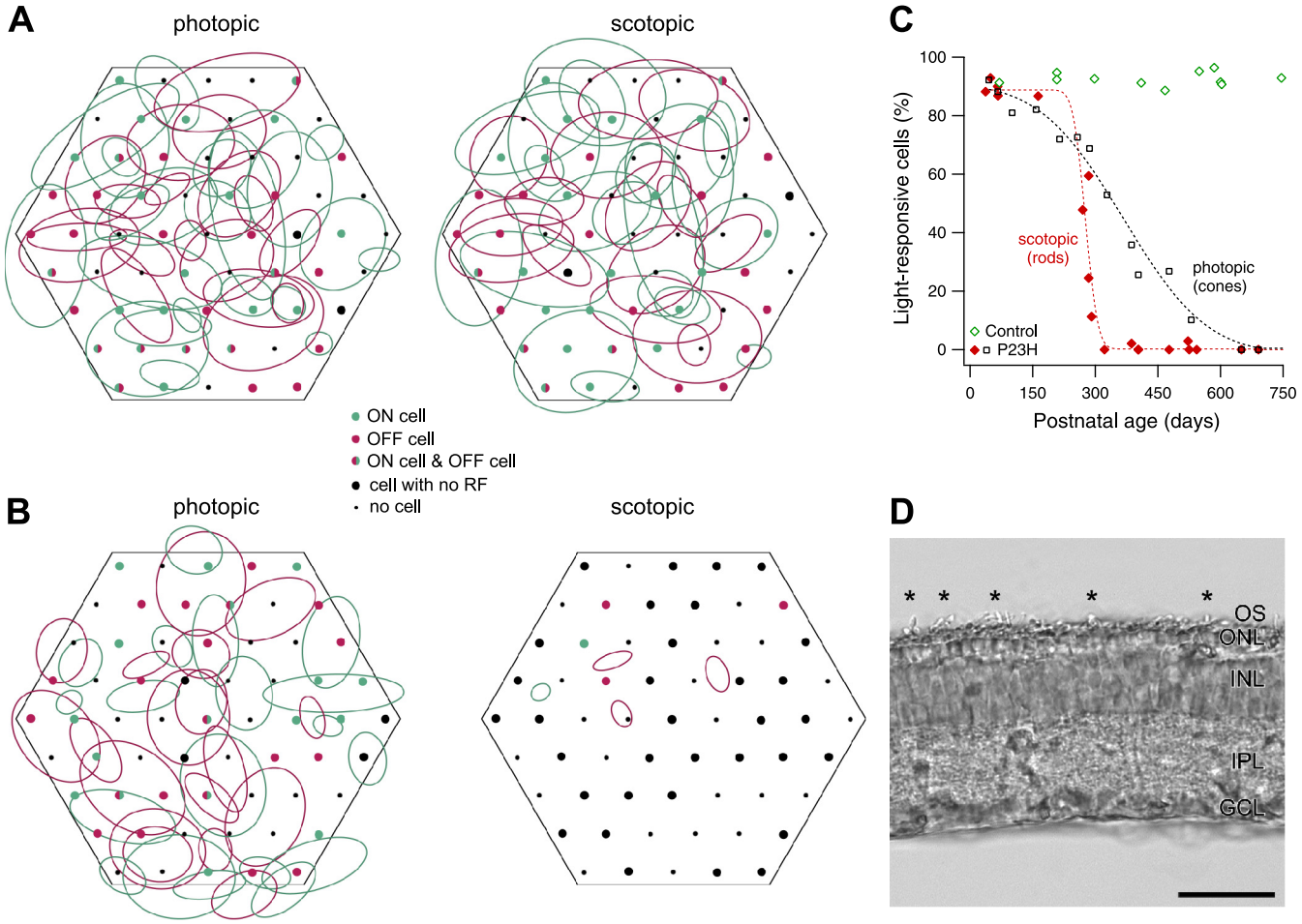

Fig. 3. Light responses mediated by cones and rods. *A*: schematic representation of the multielectrode array and RFs measured in a postnatal day (P)298 control retina. Magenta and green ellipses indicate RF outlines for all OFF and ON cells, respectively, recorded in this retina. Dots represent array electrodes; the color of the filled circles indicates whether ON cells, OFF cells, both, or neither were recorded at a given electrode location. *Left*: results from visual stimulation that favored detection of cone-mediated RFs (photopic). *Right*: same retina, but stimulated with scotopic (low-light level) visual stimuli intended to isolate rod-mediated responses. In the actual experiment, scotopic recordings preceded photopic recordings so as to avoid rod photoreceptor bleaching. *B*: RFs measured in a P291 P23H retina with the same stimuli as in *A*. Compared with the photopic condition, the low-light stimulus (scotopic) yielded a similar number of cells recorded on similar electrodes, but very few RFs. *C*: fraction of light-responsive cells recorded with rod-isolating stimuli (scotopic, red and green symbols) for all retinas tested with this stimulus. Dotted red line is a sigmoidal fit to the P23H data. Open squares and dotted black line show cone-mediated light responses (from Sekirnjak et al. 2009). *D*: retinal cross section of a P344 P23H rat. Sparse photoreceptor outer segments (OS) reminiscent of cones can be seen (asterisks) in an otherwise bare photoreceptor layer. ONL, outer nuclear layer; INL, inner nuclear layer; IPL, inner plexiform layer; GCL, ganglion cell layer. Scale bar, 50 μm.

Spontaneous Firing in ON and OFF RGCs

Several previous studies have reported that spontaneous firing in RGCs of degenerating retina is markedly elevated (e.g., Margolis et al. 2008; Stasheff 2008), but little is known about the differential contribution of the ON and OFF pathways to this hyperactivity. We measured the spontaneous activity of 220 control and 317 P23H cells under dark conditions.

Figure 4*A* shows that in control animals no systematic variation of firing rate with age was observed. Notably, ON cells exhibited significantly lower spontaneous rates (3.4 ± 0.3 Hz; $n = 87$) than OFF cells (10.8 ± 0.5; $n = 133$) ($P < 0.001$). Spontaneous activity in P23H retina is shown in Fig. 4*B*. At the earliest time points, firing rates in both ON and OFF cells were similar to those in control animals ($P > 0.6$). Between P75 and P550, however, P23H animals showed a period of vigorous hyperactivity in OFF cells, but not in ON cells. Note that since no light-responsive P23H cells could be recorded at >P600, the identity of the data points at P600–P750 could not be established with certainty. However, since the spontaneous activity in P23H ON cells (average 1.8 ± 0.2 Hz, $n = 95$) was much lower than in control retinas ($P < 0.001$) and tended to decline with age, the data points plotted as triangles in Fig. 4*B* probably primarily represent OFF cell activity.

Synaptic vs. Intrinsic Contributions to Hyperactivity

To determine whether RGC hyperactivity in degenerating P23H retina was primarily caused by changes in inputs from the retinal network, synaptic transmission was blocked pharmacologically. We opted not to use cadmium chloride because it blocks voltage-gated calcium channels on RGC somas and therefore profoundly alters spontaneous firing. Instead, a cocktail of synaptic inhibitors was applied to the bath solution: the non-NMDA glutamate receptor antagonist CNQX, the NMDA receptor antagonist APV, the metabotropic glutamate receptor agonist APB, the glycine receptor blocker strychnine, the GABA-A receptor antagonist picrotoxin, and the nonselective glutamate receptor blocker kynurenate. Application of the inhibitor cocktail abolished all light-evoked responses within several minutes in every retina tested (not shown). The blockers also eliminated long-latency responses evoked by electrical stimulation in two cells (2 ms and 6 ms), without blocking submillisecond-latency spikes (not shown), consistent with an elimination of synaptic activity.

First, Fig. 5*A*, *left*, shows the effect of the inhibitor cocktail on spontaneous firing of RGCs in four control retinas (P208, P208, P549, P746). Firing rates were reduced in 38 of 38 OFF cells (from 12 ± 1 to 5 ± 1 Hz) and 20 of 20 ON cells (from 2.6 ± 0.4 to 0.1 ± 0.1 Hz). Second, four P23H animals with ages near the period of highest elevated firing were tested (P284, P284, P291, P387). If the retinal network was the sole source of hyperactivity, synaptic blockade would be expected to diminish spontaneous OFF cell firing to values around 5 Hz, the average rate in control retinas with applied inhibitors. Results are shown in Fig. 5*A*, *right*. Firing rates were reduced in 34 of 34 OFF cells from 25 ± 2 to 15 ± 2 Hz, corresponding to ~50% of the expected drop in spontaneous firing. Firing rates were increased in 18 of 22 ON cells and slightly reduced in 4 of 22 ON cells (average: from 1.5 ± 0.3 to 3.8 ± 0.8 Hz). The absolute reduction in OFF cell firing was similar between control and P23H retinas (8 ± 1 Hz and 10 ± 1 Hz, respectively).

To test whether nonsynaptic physiology was affected by the inhibitors, Fig. 5, *B* and *C*, show the amplitude of spontaneous spikes and the results of electrical stimulation before and after inhibitor application. There was no change in spike amplitude in 58 cells from control retinas (from 308 ± 18 to 289 ± 25 μV) and 56 cells from P23H retinas (from 446 ± 26 to 441 ± 27 μV). Electrical stimulation thresholds were unchanged in 8 cells from control retinas (from 0.040 ± 0.010 to 0.044 ± 0.013 mC/cm^2) and in 18 cells from P23H retinas (from 0.052 ± 0.005 to 0.052 ± 0.004 mC/cm^2). No change in evoked spike latency was observed (data not shown). These findings therefore reveal no obvious changes in intrinsic physiology of RGCs during degeneration.

DISCUSSION

The present work reports the direct and indirect effects of photoreceptor degeneration on RGCs in the P23H-1 rat. The results reveal a variety of functional changes in RGCs during degeneration and suggest possible mechanisms.

Shrinking and Weakening of Visual Receptive Fields

During early and intermediate stages of degeneration, RGCs remained sufficiently light responsive that RFs could be mea-

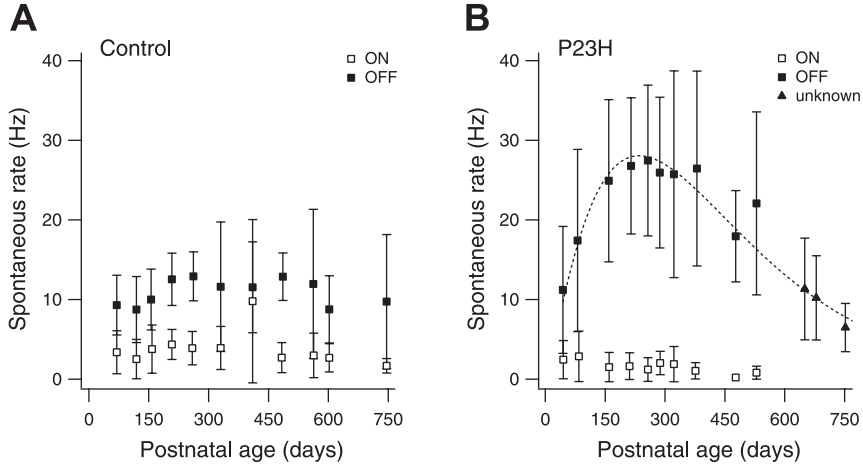

Fig. 4. Spontaneous activity in ON and OFF ganglion cells. *A*: spontaneous firing rate measured in ganglion cells of control retinas as a function of animal age. Each data point represents the average rate measured in 8 ± 1 ON cells ($n = 87$ cells) and 13 ± 1 OFF cells ($n = 133$ cells). Error bars indicate SD. *B*: spontaneous firing rate measured in ganglion cells of P23H retinas. Each data point represents the average rate measured in 9 ± 2 ON cells ($n = 95$), 18 ± 2 OFF cells ($n = 175$), and 15 ± 1 unidentified cells (unknown; $n = 47$). Error bars indicate SD. Dashed line is a fit function to all non-ON cell data points (see METHODS).

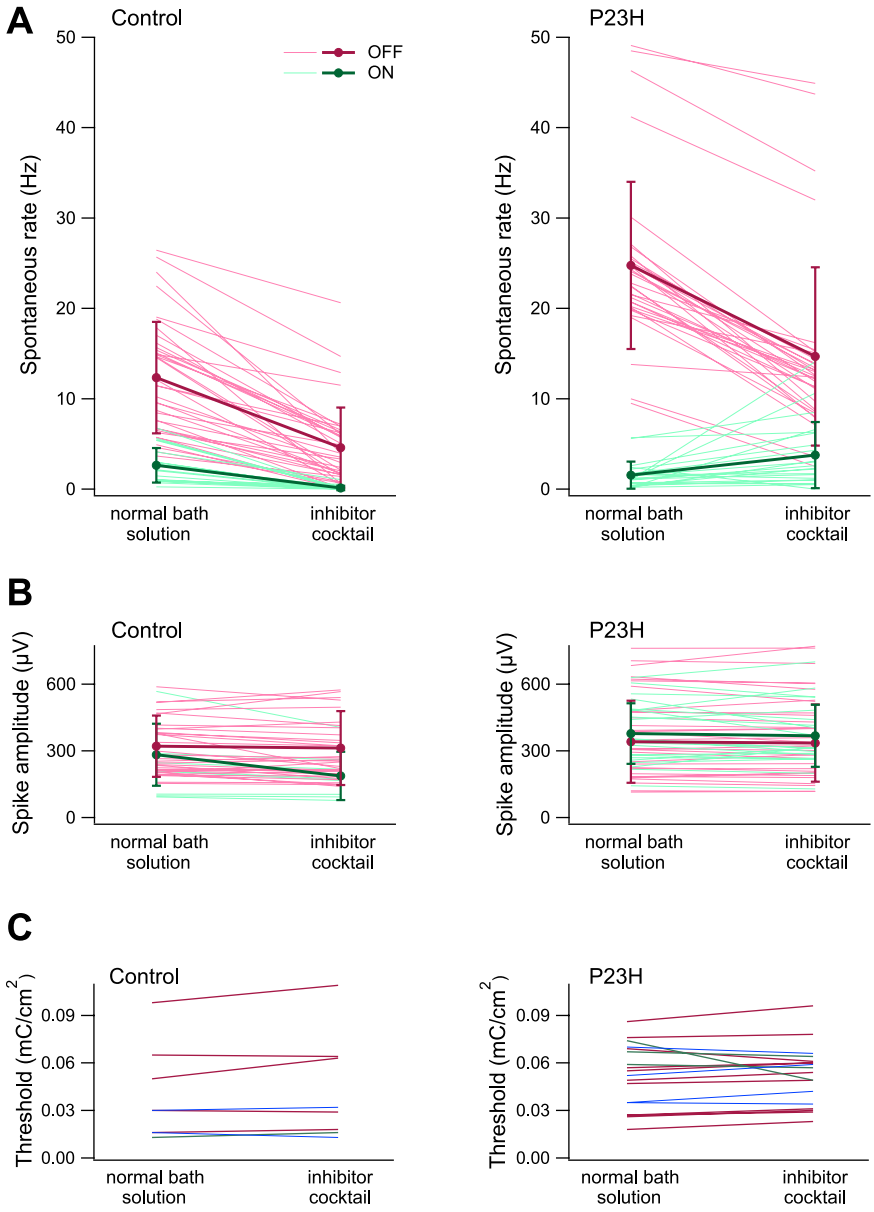

Fig. 5. Effect of synaptic inhibitors on control and P23H retina. *A*, *left*: spontaneous firing rates of ganglion cells in control retina before and after application of a synaptic inhibitor cocktail. Each thin line represents the firing rate of a single cell: 20 ON cells and 37 OFF cells from 4 animals are shown (P208, P208, P549, P746). Averages ± SD are shown by thick lines. The following inhibitors were used (in μM): 70 6-cyano-7-nitroquinoxaline-2,3-dione (CNQX), 200 2-amino-5-phosphonovaleric acid (APV), 50 2-amino-4-phosphonobutyric acid (APB), 10 strychnine, 100 picrotoxin, 1,000 kynurenate. *Right*: spontaneous firing rates of P23H ganglion cells before and after application of the inhibitor cocktail: 22 ON cells and 33 OFF cells from 4 animals are shown (P284, P284, P291, P387). *B*: spike amplitudes measured in the same set of cells as in *A*. *C*: thresholds for epiretinal stimulation of 8 ganglion cells in control retina (*left*) and 18 P23H cells (*right*) before and after application of the synaptic inhibitor cocktail. Blue lines represent cells that were not identified as ON or OFF (2 control and 4 P23H cells). One LE ON cell, 5 LE OFF cells, 3 P23H ON cells, and 11 P23H OFF cells are shown.

sured, and a decline in the strength and size of RFs was observed. Recordings in the superior colliculus of RCS rats have shown that visual sensitivities in response to light flashes are progressively reduced with age (Sauve et al. 2001, 2004). The only study reporting detailed RF properties in degenerating retina found that in RCS rats SNR and RF size decreased with advancing degeneration, as measured by stimulation with spots of light (Pu et al. 2006). The present study similarly documents an age-dependent decline in the sensitivity and size of RFs. In P23H retina, the decrease in RF diameter (to 50% from the initial level) was somewhat more pronounced than in the RCS rat (to ~70%), while the RF strength declined less severely (to 25%) than in RCS rats (to 10%). Interestingly, during the early stages of degeneration (<P300) RFs were weaker but not smaller. Subsequently, RF size declined rapidly, while RF strength changed little. The timing of the RF size change suggests a possible mechanism: the preferential loss of rod-mediated light responses (see below). Previous work in cat (Barlow et al. 1957) as well as recent work in primate retina (Field et al. 2008) indicates that rod-mediated RFs are significantly larger than cone-mediated RFs.

The time course of decline of RF diameter was similar to that of the decline in the number of light-responsive cells (Fig. 2*B* in Sekirnjak et al. 2009). This suggests that RGCs increasingly fail to be categorized as light responsive as the RF shrinks. A possible interpretation of these findings is that the strength of photoreceptor inputs decreases over time, first producing an apparently smaller RF as the weaker flanks of the RF are obscured by noise, and later a complete loss of a measurable RF.

Similar Loss of Light Responses in ON and OFF RGCs

Comparable numbers of ON and OFF cells were recorded up to P400, an age at which only ~20% of RGCs show any response to visual stimulation (Sekirnjak et al. 2009). This finding contrasts with the reported relative preservation of OFF cells in rd1 mouse retina at an intermediate stage of degeneration (Stasheff 2008). A significant difference in that study was

the use of full-field flash stimuli, which activate the antagonistic RF center and surround simultaneously, potentially weakening or reversing the polarity of light responses. Another study reported preferential loss of ON cells in RCS rat (Pu et al. 2006); however, the analysis included only cells with the largest RFs. Another possible explanation for the difference between the present and previous findings is that the low spontaneous activity of ON cells during degeneration produced a selection bias toward OFF cells for recording in previous work. Furthermore, differences in species or experimental conditions may contribute. Finally, it is possible that degeneration proceeds more symmetrically across ON and OFF cells in the P23H rat than in the other degeneration models. Consistent with this possibility, the RCS rat and the rd1 mouse differ from the P23H rat in other respects, such as primary cause, onset age, and speed of degeneration (Carter-Dawson et al. 1978; Dowling and Sidman 1962; Pu et al. 2006). These observations highlight the importance of determining which animal models are most appropriate for understanding the various forms of human retinal degeneration. Also, although the relatively large number of cells examined for light responses in this study makes a sampling bias a less likely explanation for the discrepancies (about 600 P23H cells vs. 73 in RCS rat and 243 in rd1 mouse), RGCs were not classified into distinct types. For instance, whereas there are not many types of cells exhibiting ON-OFF responses in the mammalian retina, some may appear in our recordings and may be classified as OFF cells because of the dominant OFF component in the STA. In future work, it may be valuable to examine the possibility of differential cell loss in the multiple morphologically distinct RGC types.

Cones Mediate Light Responses at Later Stages of Degeneration

Rod-mediated light responses exhibited earlier and more rapid deterioration than cone-mediated light responses. This is consistent with the evidence of long-term cone survival reported in P23H line 3 (Chrysostomou et al. 2009) and line 1 (Cuenca et al. 2004; Machida et al. 2000) rats. While the rat photoreceptor layer contains only 1–3% cones (Bertschinger et al. 2008; Cuenca et al. 2004; Szel and Rohlich 1992), cones appear to survive in sufficient numbers to generate the few small, weak RFs observed in the present study for P23H animals as old as P543. There was also anatomic evidence of surviving cones in retinal cross sections (see Fig. 3). However, the slicing method used probably induced substantial mechanical damage, and therefore was not suitable for measuring the number of surviving cones. Studies using embedded cryosections have shown that P23H-3 cone outer segments survive until late adulthood (P540), but are shortened to <10 μm (Chrysostomou et al. 2008, 2009). The finding that rod function was impaired before cone function is also consistent with clinical reports in human P23H autosomal dominant RP patients (Berson et al. 1991), who experience night blindness before other forms of vision loss.

In P23H animals, cones degenerate despite the fact that the underlying mutation is in a rod-specific protein. The mechanism of this transfer of degeneration is poorly understood. Suggestions include cone injury due to oxidative damage caused by the absence of rods (Shen et al. 2005), the spread of a toxic substance from dying rods to healthy cones through gap junctions (Ripps 2002), a rod degeneration-induced lack of a diffusible trophic factor normally released from rods stimulating cone survival (Mohand-Said et al. 1998), and cone damage due to a decline in renewal of structural proteins (John et al. 2000). Interestingly, there is evidence from homozygous P23H-1 rats that after rods have degenerated, surviving cones synapse onto both rod and cone bipolar cells (Cuenca et al. 2004).

Spontaneous Firing and Hyperactivity in ON and OFF Cells

Spontaneous firing differed between ON and OFF cells, in both control and P23H rats. In control rats, the spontaneous firing rate of OFF cells in darkness was higher than that of ON cells. This resembles findings in other species, including primates (e.g., Barlow and Levick 1969; Myhr et al. 2001; Northmore and Oh 1998; Rizzo 2004; Uzzell 2005), but contrasts with results in wild-type mice, in which no difference was found (Margolis and Detwiler 2007; Qu and Myhr 2008; Stasheff 2008). In degenerating P23H retina, OFF cells (but not ON cells) exhibited strongly elevated firing at early and intermediate ages. Periods of physiological hyperactivity have been observed in all model species and strains with outer retinal degeneration studied thus far: RCS rat (Pu et al. 2006; Sauve et al. 2001), rd1/C57 mouse (Dräger and Hubel 1978; Stasheff 2008), rd1 mouse (Margolis et al. 2008; Stasheff 2008), and P23H rat (Sekirnjak et al. 2009). However, the restriction of hyperactivity to OFF cells contrasts with results from the rd1 mouse, in which both ON and OFF cells exhibited increased spontaneous firing (Margolis et al. 2008; Stasheff 2008), albeit with the largest increase in OFF cells (Margolis et al. 2008). It should be noted that in the rd1 model outer retinal degeneration occurs earlier than in P23H retina, which may perturb the development of the mechanisms of spontaneous firing. Specifically, the rapid loss of photoreceptors during an early developmental period may disrupt developmental plasticity and ganglion cell dendritic segregation, resulting in an abnormal balance of excitatory-to-inhibitory inputs to ganglion cells (see Stasheff 2008). Note also that in the study of Margolis et al. (2008) only ganglion cells with the largest soma diameters were targeted, whereas the present study is based on a more heterogeneous ganglion cell population.

ON and OFF cells also differed in the relative contribution of synaptic activity to spontaneous firing. Like other neurons in the CNS (Harris-Warrick 2002; Hausser et al. 2004; Lin and Carpenter 1993), RGCs are intrinsically active and spontaneous firing is modulated by tonic synaptic inputs (Margolis and Detwiler 2007), both inhibitory (amacrine) and excitatory (bipolar). The pharmacological blockade (see Fig. 5) isolated RGCs from their inputs and removed the effect of elevated free glutamate levels associated with degeneration (Delyfer et al. 2005); it should be noted, however, that our inhibitor cocktail did not block inputs from cholinergic starburst amacrine cells (Brecha et al. 1988), whose role in the adult retina remains poorly understood (see, e.g., Famiglietti and Sundquist 2010; Masland 2005). In OFF cells, the pharmacological manipulation decreased firing rates by similar amounts in control and P23H retinas. However, this reduction ($\sim$10 Hz) was lower than the decrease expected ($\sim$20 Hz) if the retinal network were the only source of elevated firing (see Fig. 5). Thus synaptic activity accounted for only about half of the observed

hyperactivity. Although the effect of blocking synaptic transmission on spontaneous firing rates has not been directly tested in other degenerative animal models, it appears that hyperactivity in rd1 mouse RGCs is almost always generated extrinsically (Margolis and Detwiler 2011): the membrane fluctuations underlying spontaneous activity in voltage-clamped cells were reduced >90% after synaptic blocker applications (Margolis et al. 2008). In contrast to OFF cells, spontaneous firing in ON cells largely ceased in control retina, but increased in P23H retina after application of synaptic blockers. The changes, however, were small and variable. The observed ON-OFF asymmetry is consistent with the previous finding that ON and OFF cells differ in their intrinsic membrane properties (Margolis and Detwiler 2007).

At late stages of degeneration, spontaneous firing rates in OFF cells returned to values at or below those found in control animals. A similar observation has been recently reported in albino P23H rats: firing rates were moderately lower in >1-year-old animals that did not show any remaining visual function (Kolomiets et al. 2010). Note that albino P23H rats display a faster degeneration time course than pigmented animals (Lowe et al. 2005; Sekirnjak et al. 2009): the age at which all visual function is lost corresponds to ~19 mo in the present study and ~12 mo in the albino study. Similarly, firing rates in the rd1 mouse decrease at late degenerative stages (Margolis et al. 2008). It is tempting to speculate that RGC hyperactivity underlies the observation that human RP patients commonly report spontaneous percepts at intermediate stages of RP progression but not during early or late phases of the disease (Delbeke et al. 2001; Heckenlively et al. 1988).

A Time Course Summary of Degeneration

Figure 6 shows seven normalized parameters that summarize the time course of degeneration in pigmented P23H retina. Several distinct periods emerge.

The earliest manifestations of outer retinal degeneration on visual function (before P100) are the sharp decrease in retinal thickness and the decline in RF strength. Notably, these changes occur before significant changes in the number of light-responsive cells, whether rod- or cone mediated: despite a much reduced photoreceptor layer, RFs are unaltered in number and size. This delayed loss of responsive cells is consistent with ERG recordings in P23H rats, which showed significant changes only after the outer nuclear layer had thinned beyond 50% (Chrysostomou et al. 2009; Machida et al. 2000). At around the same time, spontaneous firing rates begin to increase sharply.

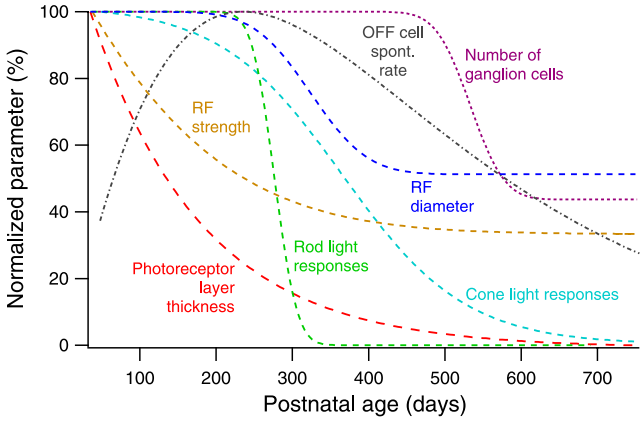

Fig. 6. Events associated with degeneration in P23H rat. Comparison of time courses of anatomic, physiological, and light-evoked retinal parameters in P23H retina. Dashed lines are fit functions to the indicated parameters from the present study and our prior study (Sekirnjak et al. 2009). All data were normalized to the maximum value. Rod and cone light responses refer to the relative number of light-responsive cells measured. The RF strength time course shown here is a combined average for all ON and OFF cells (plotted separately in Fig. 1*D*).

Multiple changes occur between P100 and P350. As the photoreceptor layer thickness falls below 20%, rod-mediated light responses mostly disappear. Cone-mediated responses remain, albeit with diminished RF strength and size. During this period, OFF RGCs also attain their maximum firing rates.

The next time period (P350–P500) is characterized by further reduction of RF diameter but no change in RF strength. Eventually, light responses are lost as the photoreceptor layer disappears. The number of recorded RGCs remains roughly normal.

In the final phase (P500–P750), an essentially blind retina undergoes loss of recordable RGCs, while the spontaneous activity of the remaining cells falls below control levels. This period may correspond to the retinal restructuring known as "phase 3 remodeling" (Jones et al. 2003).

ACKNOWLEDGMENTS

We thank Matthew LaVail and Chrysalis DNX Transgenic Sciences (Princeton, NJ) for providing the P23H breeding animals to establish our colony. We also thank Greg Field for the photon flux measurements.

GRANTS

This research was supported by the Salk Institute Pioneer Postdoctoral Fellowship, Second Sight Medical Products Inc. (SSMP), NEI Grants EY-018003 (E. J. Chichilnisky) and EY-012893 (SSMP), National Science Foundation Award PHY-0417175 and NIH Grant R21-EB-004410 (A. M. Litke), Burroughs Wellcome Fund Career Award at Scientific Interfaces (A. Sher), and the Polish Ministry of Science and Higher Education (W. Dabrowski).

DISCLOSURES

No conflicts of interest, financial or otherwise, are declared by the author(s).

REFERENCES

Barlow HB, Fitzhugh R, Kuffler SW. Change of organization in the receptive fields of the cat's retina during dark adaptation. *J Physiol* 137: 338–354, 1957.

Barlow HB, Levick WR. Changes in the maintained discharge with adaptation level in the cat retina. *J Physiol* 202: 699–718, 1969.

Berson EL, Rosner B, Sandberg MA, Dryja TP. Ocular findings in patients with autosomal dominant retinitis pigmentosa and a rhodopsin gene defect (Pro-23-His). *Arch Ophthalmol* 109: 92–101, 1991.

Bertschinger DR, Beknazar E, Simonutti M, Safran AB, Sahel JA, Rosolen SG, Picaud S, Salzmann J. A review of in vivo animal studies in retinal prosthesis research. *Graefes Arch Clin Exp Ophthalmol* 246: 1505–1517, 2008.

Brecha N, Johnson D, Peichl L, Wassle H. Cholinergic amacrine cells of the rabbit retina contain glutamate decarboxylase and gamma-aminobutyrate immunoreactivity. *Proc Natl Acad Sci USA* 85: 6187–6191, 1988.

Carter-Dawson LD, LaVail MM, Sidman RL. Differential effect of the rd mutation on rods and cones in the mouse retina. *Invest Ophthalmol Vis Sci* 17: 489–498, 1978.

Chader GJ, Weiland J, Humayun MS. Artificial vision: needs, functioning, and testing of a retinal electronic prosthesis. *Prog Brain Res* 175: 317–332, 2009.

Chichilnisky EJ. A simple white noise analysis of neuronal light responses. *Network* 12: 199–213, 2001.

Chichilnisky EJ, Kalmar RS. Functional asymmetries in ON and OFF ganglion cells of primate retina. *J Neurosci* 22: 2737–2747, 2002.

Chrysostomou V, Stone J, Stowe S, Barnett NL, Valter K. The status of cones in the rhodopsin mutant P23H-3 retina: light-regulated damage and repair in parallel with rods. *Invest Ophthalmol Vis Sci* 49: 1116–1125, 2008.

Chrysostomou V, Stone J, Valter K. Life history of cones in the rhodopsin-mutant P23H-3 rat: evidence of long-term survival. *Invest Ophthalmol Vis Sci* 50: 2407–2416, 2009.

Cicerone CM, Green DG, Fisher LJ. Cone inputs to ganglion cells in hereditary retinal degeneration. *Science* 203: 1113–1115, 1979.

Cuenca N, Pinilla I, Sauve Y, Lu B, Wang S, Lund RD. Regressive and reactive changes in the connectivity patterns of rod and cone pathways of P23H transgenic rat retina. *Neuroscience* 127: 301–317, 2004.

Delbeke J, Pins D, Michaux G, Wanet-Defalque MC, Parrini S, Veraart C. Electrical stimulation of anterior visual pathways in retinitis pigmentosa. *Invest Ophthalmol Vis Sci* 42: 291–297, 2001.

Delyfer MN, Forster V, Neveux N, Picaud S, Leveillard T, Sahel JA. Evidence for glutamate-mediated excitotoxic mechanisms during photoreceptor degeneration in the rd1 mouse retina. *Mol Vis* 11: 688–696, 2005.

Dowling JE, Sidman RL. Inherited retinal dystrophy in the rat. *J Cell Biol* 14: 73–109, 1962.

Dräger UC, Hubel DH. Studies of visual function and its decay in mice with hereditary retinal degeneration. *J Comp Neurol* 180: 85–114, 1978.

Famiglietti EV, Sundquist SJ. Development of excitatory and inhibitory neurotransmitters in transitory cholinergic neurons, starburst amacrine cells, and GABAergic amacrine cells of rabbit retina, with implications for previsual and visual development of retinal ganglion cells. *Vis Neurosci* 27: 19–42, 2010.

Field GD, Gauthier JL, Greschner M, Shlens J, Sher A, Litke AM, Chichilnisky EJ. Light adaptation changes the size of receptive fields in seven distinct primate retinal ganglion cell types. *Invest Ophthalmol Vis Sci* 49: ARVO Abstract 3856, 2008.

Field GD, Greschner M, Gauthier JL, Rangel C, Shlens J, Sher A, Marshak DW, Litke AM, Chichilnisky EJ. High-sensitivity rod photoreceptor input to the blue-yellow color opponent pathway in macaque retina. *Nat Neurosci* 12: 1159–1164, 2009.

Harris-Warrick RM. Voltage-sensitive ion channels in rhythmic motor systems. *Curr Opin Neurobiol* 12: 646–651, 2002.

Hausser M, Raman IM, Otis T, Smith SL, Nelson A, du Lac S, Loewenstein Y, Mahon S, Pennartz C, Cohen I, Yarom Y. The beat goes on: spontaneous firing in mammalian neuronal microcircuits. *J Neurosci* 24: 9215–9219, 2004.

Heckenlively JR, Yoser SL, Friedman LH, Oversier JJ. Clinical findings and common symptoms in retinitis pigmentosa. *Am J Ophthalmol* 105: 504–511, 1988.

Javaheri M, Hahn DS, Lakhanpal RR, Weiland JD, Humayun MS. Retinal prostheses for the blind. *Ann Acad Med Singapore* 35: 137–144, 2006.

John SK, Smith JE, Aguirre GD, Milam AH. Loss of cone molecular markers in rhodopsin-mutant human retinas with retinitis pigmentosa. *Mol Vis* 6: 204–215, 2000.

Jones BW, Marc RE. Retinal remodeling during retinal degeneration. *Exp Eye Res* 81: 123–137, 2005.

Jones BW, Watt CB, Frederick JM, Baehr W, Chen CK, Levine EM, Milam AH, Lavail MM, Marc RE. Retinal remodeling triggered by photoreceptor degenerations. *J Comp Neurol* 464: 1–16, 2003.

Kolomiets B, Dubus E, Simonutti M, Rosolen S, Sahel JA, Picaud S. Late histological and functional changes in the P23H rat retina after photoreceptor loss. *Neurobiol Dis* 38: 47–58, 2010.

Lin Y, Carpenter DO. Medial vestibular neurons are endogenous pacemakers whose discharge is modulated by neurotransmitters. *Cell Mol Neurobiol* 13: 601–613, 1993.

Litke AM. The retinal readout system: an application of microstrip detector technology to neurobiology. *Nucl Instrum Methods Phys Res A* 418: 203–209, 1998.

Litke AM, Bezayiff N, Chichilnisky EJ, Cunningham W, Dabrowski W, Grillo AA, Grivich M, Grybos P, Hottowy P, Kachiguine S, Kalmar RS, Mathieson K, Petrusca D, Rahman M, Sher A. What does the eye tell the brain? Development of a system for the large scale recording of retinal output activity. *IEEE Trans Nucl Sci* 51: 1434–1440, 2004.

Litke AM, Chichilnisky EJ, Dabrowski W, Grillo AA, Grybos P, Kachiguine S, Rahman M, Taylor G. Large-scale imaging of retinal output activity. *Nucl Instrum Methods Phys Res A* 501: 298–307, 2003.

Lowe RJ, Duncan JL, Yang H, Donohue-Rolfe KM, Matthes MT, Yasumura D, LaVail MM. Retinal degeneration is slowed by eye pigmentation in P23H but not in S334ter mutant rhodopsin transgenic rats. *Invest Ophthalmol Vis Sci* 46: ARVO Abstract 2300, 2005.

Machida S, Kondo M, Jamison JA, Khan NW, Kononen LT, Sugawara T, Bush RA, Sieving PA. P23H rhodopsin transgenic rat: correlation of retinal function with histopathology. *Invest Ophthalmol Vis Sci* 41: 3200–3209, 2000.

Marc RE, Jones BW, Anderson JR, Kinard K, Marshak DW, Wilson JH, Wensel T, Lucas RJ. Neural reprogramming in retinal degeneration. *Invest Ophthalmol Vis Sci* 48: 3364–3371, 2007.

Margolis DJ, Detwiler PB. Different mechanisms generate maintained activity in ON and OFF retinal ganglion cells. *J Neurosci* 27: 5994–6005, 2007.

Margolis DJ, Newkirk G, Euler T, Detwiler PB. Functional stability of retinal ganglion cells after degeneration-induced changes in synaptic input. *J Neurosci* 28: 6526–6536, 2008.

Margolis DJ, Detwiler PB. Cellular origin of spontaneous ganglion cell spike activity in animal models of retinitis pigmentosa. *J Ophthalmol* 2011: 507037, 2011.

Masland RH. The many roles of starburst amacrine cells. *Trends Neurosci* 28: 395–396, 2005.

Mohand-Said S, Deudon-Combe A, Hicks D, Simonutti M, Forster V, Fintz AC, Leveillard T, Dreyfus H, Sahel JA. Normal retina releases a diffusible factor stimulating cone survival in the retinal degeneration mouse. *Proc Natl Acad Sci USA* 95: 8357–8362, 1998.

Mokwa W, Goertz M, Koch C, Krisch I, Trieu HK, Walter P. Intraocular epiretinal prosthesis to restore vision in blind humans. *Conf Proc IEEE Eng Med Biol Soc* 2008: 5790–5793, 2008.

Myhr KL, Lukasiewicz PD, Wong RO. Mechanisms underlying developmental changes in the firing patterns of ON and OFF retinal ganglion cells during refinement of their central projections. *J Neurosci* 21: 8664–8671, 2001.

Naarendorp F, Esdaille TM, Banden SM, Andrews-Labenski J, Gross OP, Pugh ENJ. Dark light, rod saturation, and the absolute and incremental sensitivity of mouse cone vision. *J Neurosci* 30: 12495–12507, 2010.

Northmore DP, Oh DJ. Axonal conduction velocities of functionally characterized retinal ganglion cells in goldfish. *J Physiol* 506: 207–217, 1998.

Pu M, Xu L, Zhang H. Visual response properties of retinal ganglion cells in the Royal College of Surgeons dystrophic rat. *Invest Ophthalmol Vis Sci* 47: 3579–3585, 2006.

Qu J, Myhr KL. The development of intrinsic excitability in mouse retinal ganglion cells. *Dev Neurobiol* 68: 1196–1212, 2008.

Ripps H. Cell death in retinitis pigmentosa: gap junctions and the "bystander" effect. *Exp Eye Res* 74: 327–336, 2002.

Rizzo JF. Embryology, anatomy, and physiology of the afferent visual pathway. In: *Clinical Neuro-Ophthalmology*, edited by Miller NR, Newman NJ, Biousse V, Kerrison JB. Philadelphia, PA: Lippincott Williams & Wilkins, 2004, p. 3–82.

Rodieck RW. *The First Steps in Seeing*. Sunderland, MA: Sinauer, 1998.

Salzmann J, Linderholm OP, Guyomard JL, Paques M, Simonutti M, Lecchi M, Sommerhalder J, Dubus E, Pelizzone M, Bertrand D, Sahel J, Renaud P, Safran AB, Picaud S. Subretinal electrode implantation in the P23H rat for chronic stimulations. *Br J Ophthalmol* 90: 1183–1187, 2006.

Sauve Y, Girman SV, Wang S, Lawrence JM, Lund RD. Progressive visual sensitivity loss in the Royal College of Surgeons rat: perimetric study in the superior colliculus. *Neuroscience* 103: 51–63, 2001.

Sauve Y, Lu B, Lund RD. The relationship between full field electroretinogram and perimetry-like visual thresholds in RCS rats during photoreceptor degeneration and rescue by cell transplants. *Vision Res* 44: 9–18, 2004.

Schnapf JL, Kraft TW, Baylor DA. Spectral sensitivity of human cone photoreceptors. *Nature* 325: 439–441, 1987.

Schnapf JL, Nunn BJ, Meister M, Baylor DA. Visual transduction in cones of the monkey *Macaca fascicularis*. *J Physiol* 427: 681–713, 1990.

Sekirnjak C, Hottowy P, Sher A, Dabrowski W, Litke AM, Chichilnisky EJ. Electrical stimulation of mammalian retinal ganglion cells with multielectrode arrays. *J Neurophysiol* 95: 3311–3327, 2006.

Sekirnjak C, Hottowy P, Sher A, Dabrowski W, Litke AM, Chichilnisky EJ. High-resolution electrical stimulation of primate retina for epiretinal implant design. *J Neurosci* 28: 4446–4456, 2008.

Sekirnjak C, Hulse C, Jepson LH, Hottowy P, Sher A, Dabrowski W, Litke AM, Chichilnisky EJ. Loss of responses to visual but not electrical

stimulation in ganglion cells of rats with severe photoreceptor degeneration. *J Neurophysiol* 102: 3260–3269, 2009.

Shen J, Yang X, Dong A, Petters RM, Peng YW, Wong F, Campochiaro PA. Oxidative damage is a potential cause of cone cell death in retinitis pigmentosa. *J Cell Physiol* 203: 457–464, 2005.

Stasheff SF. Emergence of sustained spontaneous hyperactivity and temporary preservation of OFF responses in ganglion cells of the retinal degeneration (rd1) mouse. *J Neurophysiol* 99: 1408–1421, 2008.

Szel A, Rohlich P. Two cone types of rat retina detected by anti-visual pigment antibodies. *Exp Eye Res* 55: 47–52, 1992.

Uzzell VJ. *Sensitivity and Noise in Primate Retinal Ganglion Cells* (PhD dissertation). Neuroscience Program, University of California, San Diego, 2005.

Waxman SG, Dib-Hajj S, Cummins TR, Black JA. Sodium channels and their genes: dynamic expression in the normal nervous system, dysregulation in disease states (1). *Brain Res* 886: 5–14, 2000.

Winter JO, Cogan SF, Rizzo JF. Retinal prostheses: current challenges and future outlook. *J Biomater Sci Polym Ed* 18: 1031–1055, 2007.

Yanai D, Weiland JD, Mahadevappa M, Greenberg RJ, Fine I, Humayun MS. Visual performance using a retinal prosthesis in three subjects with retinitis pigmentosa. *Am J Ophthalmol* 143: 820–827, 2007.

Yang Y, Mohand-Said S, Danan A, Simonutti M, Fontaine V, Clerin E, Picaud S, Leveillard T, Sahel JA. Functional cone rescue by RdCVF protein in a dominant model of retinitis pigmentosa. *Mol Ther* 17: 787–795, 2009.

Yin L, Smith RG, Sterling P, Brainard DH. Chromatic properties of horizontal and ganglion cell responses follow a dual gradient in cone opsin expression. *J Neurosci* 26: 12351–12361, 2006.

Zrenner E, Wilke R, Bartz-Schmidt K, Benav H, Besch D, Gekeler F, Koch J, Porubská K, Sachs H, Wilhelm B. Blind retinitis pigmentosa patients can read letters and recognize the direction of fine stripe patterns with subretinal electronic implants. *Invest Ophthalmol Vis Sci* 50: E-Abstract 4581, 2009.